European Journal of Heart Failure (2011) **13**, 1275–1282
doi:10.1093/eurjhf/hfr134

Differential responses of the right ventricle to abnormal loading conditions in mice: pressure vs. volume load

Beatrijs Bartelds[1,2]*, Marinus A. Borgdorff[1,2], Annemiek Smit-van Oosten[1], Janny Takens[1,2], Bibiche Boersma[1,2], Marcel G. Nederhoff[3], Nynke J. Elzenga[1], Wiek H. van Gilst[2], Leon J. De Windt[4], and Rolf M.F. Berger[1,2]

[1]Department of Pediatric Cardiology, Center for Congenital Heart Disease, Beatrix Children's Hospital, University Medical Center Groningen, Rm W4.189, CA41, Hanzeplein 1, 9700 RB Groningen, The Netherlands; [2]Cardiovascular Research Center, GUIDE, University Medical Center Groningen, Groningen, The Netherlands; [3]Department of Medical Physiology, Division Heart & Lungs, University Medical Center Utrecht, Utrecht, The Netherlands; and [4]Department of Cardiology, Cardiovascular Research Institute, University of Maastricht, Maastricht, The Netherlands

Received 19 March 2011; revised 30 June 2011; accepted 8 July 2011; online publish-ahead-of-print 24 October 2011

Aims Right ventricular (RV) dysfunction is a major determinant of long-term morbidity and mortality in congenital heart disease. The right ventricle (RV) is genetically different from the left ventricle (LV), but it is unknown as to whether this has consequences for the cellular responses to abnormal loading conditions. In the LV, calcineurin-activation is a major determinant of pathological hypertrophy and an important target for therapeutic strategies. We studied the functional and molecular adaptation of the RV in mouse models of pressure and volume load, focusing on calcineurin-activation.

Methods and results Mice were subjected to pulmonary artery banding (PAB), aorto-caval shunt (Shunt), or sham surgery (Control). Four weeks later, mice were functionally evaluated with cardiac magnetic resonance imaging, pressure measurements, and voluntary cage wheel exercise. Right ventricular hypertrophy and calcineurin-activation were assessed after sacrifice. Mice with increased pressure load (PAB) or volume load (Shunt) of the RV developed similar degrees of hypertrophy, yet revealed different functional and molecular adaptation. Pulmonary artery banding increased expression of Modulatory-Calcineurin-Interacting-Protein 1 (MCIP1), indicating calcineurin-activation, and the ratio of beta/alpha-Myosin Heavy Chain (MHC). In addition, PAB reduced exercise capacity and induced moderate RV dilatation with normal RV output at rest. In contrast, Shunt did not increase MCIP1 expression, and only moderately increased beta/alpha-MHC ratio. Shunt did not affect exercise capacity, but increased RV volumes and output at rest.

Conclusions Pressure and volume load induced different functional and molecular adaptations in the RV. These results may have important consequences for therapeutic strategies to prevent RV failure in the growing population of adults with congenital heart disease.

Keywords Congenital heart disease • Remodelling • Right ventricle • Hypertrophy • Pulmonary artery banding • Aorto-caval shunt

Introduction

Congenital heart disease has been treated with increasing success rates in recent years. However, long-term outcome in congenital heart disease is characterized by increasing rates of morbidity and mortality.[1–3] Right ventricular (RV) dysfunction has been shown to be an important determinant of long-term outcome.[2] The RV is frequently subjected to longstanding abnormal loading conditions as pressure or volume load in congenital heart disease. Examples of these abnormal loading conditions include: residual lesions after repair of tetralogy of Fallot (e.g. pulmonary stenosis and/or pulmonary insufficiency) or the RV as the systemic

* Corresponding author. Tel: +31 50 361 2800, Fax: +31 50 361 4235, Email: b.bartelds@umcg.nl

ventricle in congenitally corrected transposition or in univentricular circulation such as in hypoplastic left heart syndrome. Moreover, RV dysfunction predicts mortality in chronic heart failure.[4] The mechanisms of RV dysfunction and RV failure are as yet unknown. In fact, the mechanisms of RV adaptation to abnormal loading conditions are poorly understood and have not been extensively studied to date.[5]

In adults without congenital heart disease, left ventricular (LV) dysfunction is the most prominent cardiovascular disease and hence LV responses to abnormal loading conditions have been extensively studied. In the LV, calcineurin-activation is a key activator of pathological hypertrophy,[6] and interference with calcineurin-activation has been shown to reduce LV hypertrophy and improve outcome.[7] However, knowledge obtained from studies on LV adaptation cannot be directly transferred to the RV, since the RV is morphologically[8] and genetically[9] different from the LV. The RV myocardium is derived from a different set of precursor cells, the so-called anterior heart field.[10] Whether differences in genetic make-up lead to different responses to common stressors is a matter of debate.[11] Moreover, the RV is functionally different as it is coupled to the low-resistance pulmonary vasculature.[12] Differences in the genetic make-up, morphology, and functional environment suggest that the RV response to abnormal loading conditions may differ from that of the LV.

In order to understand RV adaptation, models of RV abnormal loading conditions have been developed. So far, models of pressure load in the rat and larger animals prevail.[13,14] However, genetically engineered animals will facilitate the study of the molecular pathways involved in the induction of compensatory RV hypertrophy as well as in the transition to RV failure. Hence, the need for mouse models of RV abnormal loading conditions is emerging. In these mouse models molecular pathways can be coupled to clinically relevant functional adaptation, such as exercise capacity, haemodynamics, and cardiac magnetic resonance imaging (MRI).

In this study, we compared the functional and molecular adaptation to abnormal loading conditions of the RV in two mouse models relevant for clinical lesions seen in congenital heart disease, i.e. increased pressure or volume load.

Methods

C57Bl6 mice, purchased from Harlan (Harlan, The Netherlands) were used. Animal care and experiments were conducted according to the Dutch Animal Experimental Act. The investigation conformed to the Guide for Care and Use of Laboratory Animals published by the US National Institutes of Health (NIH publication No. 85-23, revised 1996).

Surgery

Mice weighing 18–20 g underwent surgery as described in the online supplement. In short:

Pulmonary artery banding

Following left lateral thoracotomy a 7-0 suture was placed around the pulmonary artery and tied over a 23G needle bent into an L-shape.[15] The L-shaped needle was then removed and the thorax and skin were closed in layers. Mice undergoing sham thoracotomy served as controls (Control).

Aorto-caval shunt (Shunt)

Following mid-line laparotomy, a puncture was made with a 25G needle through the abdominal aorta towards the inferior caval vein while compressing the distal vein.[16,17] The puncture site in the aorta was closed with tissue glue.[16,17] The abdomen was closed in layers. Mice undergoing sham laparotomy served as controls.

We evaluated 10 mice for pulmonary artery banding (PAB), 12 for Shunt, and 10 sham-operated mice for PAB and 12 sham-operated mice for Shunt. Since there were no differences between the two groups of sham-operated animals we grouped these together and referred to them as Control.

Voluntary cage wheel exercise

Exercise capacity was tested with voluntary cage wheel exercise[18] before and 3 weeks after surgery in eight Control mice, five Shunt mice, and four PAB mice as described in the online supplementary methods.

Cardiac magnetic resonance imaging

Cardiac MRI was performed 4 weeks after surgery using a 9.4 T magnet (Bruker, Mouse MRI Facility, Interuniversity Cardiology Institute of the Netherlands). We performed cardiac MRI in five Control mice, six Shunt mice, and six PAB mice. These mice were not used for exercise studies. A detailed description of the MRI procedure is given in the online supplementary methods. The acquired cine MRI data were analysed with Qmass digital imaging software for rodents (Medis, Leiden, The Netherlands). Right ventricular end-diastolic volume (EDV) and end-systolic volume (ESV) as well as LV EDV and ESV were measured. From these volumes, stroke volume (SV), ejection fraction (EF), and RV output were calculated. Stroke work was

Table 1 Haemodynamic and magnetic resonance imaging data

	Control	PAB	Shunt
pRV systolic (mmHg)	17 ± 2	37 ± 9*	14 ± 1
Cardiac MRI			
Body weight (g)	22.7 ± 3.2	24.9 ± 1.7	26.4 ± 1.8
RV hypertrophy (mg/g)	0.94 ± 0.17	1.48 ± 0.23*	1.56 ± 0.28*
Heart rate (b.p.m.)	404 ± 40	376 ± 49	446 ± 58†
RV			
SV (μL)	20 ± 3	24 ± 5	43 ± 10*,†
Output (mL/min)	8.1 ± 1.0	8.9 ± 0.7	20.0 ± 6.2*,†
Mass (mg)	34 ± 5	61 ± 9*	62 ± 12*
EF (%)	68 ± 4	62 ± 6	58 ± 9*
LV			
EDV (μL)	45 ± 9	45 ± 7	70 ± 14*,†
ESV (μL)	19 ± 5	20 ± 8	29 ± 7*,†
SV (μL)	26 ± 5	26 ± 4	41 ± 9*,†
Output (mL/min)	10.2 ± 2.2	9.4 ± 0.7	19.4 ± 6.7*,†
Mass (mg)	69 ± 8	60 ± 5	98 ± 19*,†
EF (%)	57 ± 6	58 ± 12	59 ± 7

RV, right ventricle; LV, left ventricle; RV hypertrophy was calculated as the ratio of RV free wall weight and RV body weight; EDV, end-diastolic volume; ESV, end-systolic volume; SV, stroke volume; EF, ejection fraction. $N = 5$ for Control, 6 for Shunt, and 6 for PAB for MRI data; for RV pressures, $n = 3$ in each group. *$P < 0.05$ vs. Control, †$P < 0.05$ vs. PAB.

calculated as [(RV systolic pressure−RV diastolic pressure)×SV] and wall stress as (RV systolic pressure×RVEDV)/RV ED mass. The combined data sets of the pressure measurements and MRI measurements were used to create virtual pressure−volume loops.

Haemodynamics

Right ventricular pressures were measured invasively under anaesthesia in three Control, three Shunt, and three PAB mice 4 weeks after surgery with a fluid-filled polyurethane catheter (outer diameter 1.6, inner diameter 0.3), inserted via the jugular vein.

Tissue analysis

After the last study, the mice were sacrificed under anaesthesia (with 2−3% isoflurane and oxygen). The right ventricular free wall (RV free wall), interventricular septum (S), and left ventricular free wall (LV free wall) were separated, weighed, and stored at −80°C for further analysis. Gene and protein expression were determined as described in detail in the online supplementary methods.

Statistics

Data are presented as mean ± standard error of the mean (SEM). Differences between groups were detected with one-way analysis of variance and *post-hoc* least significant difference test (with the use of SPSS 16.0 software). A *P*-value <0.05 was considered significant. Sham-operated mice for the PAB and Shunt procedures were equal and pooled and served as controls for all surgical procedures.

Results

Functional adaptation

Pressure load, via PAB, induced an increase in peak-systolic RV pressure, whereas volume load, via Shunt, did not affect RV pressures (*Table 1*, *Figure 1A*). Three weeks after surgery, PAB mice spent significantly less time in the wheel as compared with Shunt or Control mice (*Figure 1B*). At baseline, before surgery, there were no significant differences in time spent in the wheel between PAB, Shunt, and Control mice. Wheel speed did not change in the different groups between baseline and 3 weeks after surgery, and so the time in the wheel was directly correlated with covered distance.

Mice with a pressure-loaded RV (PAB) had mild RV dilatation as shown by increased end-diastolic and end-systolic RV volumes (*Figure 1C*), whereas RV SV, output and EF were preserved when compared with Control mice (*Table 1*). Mice with a volume load

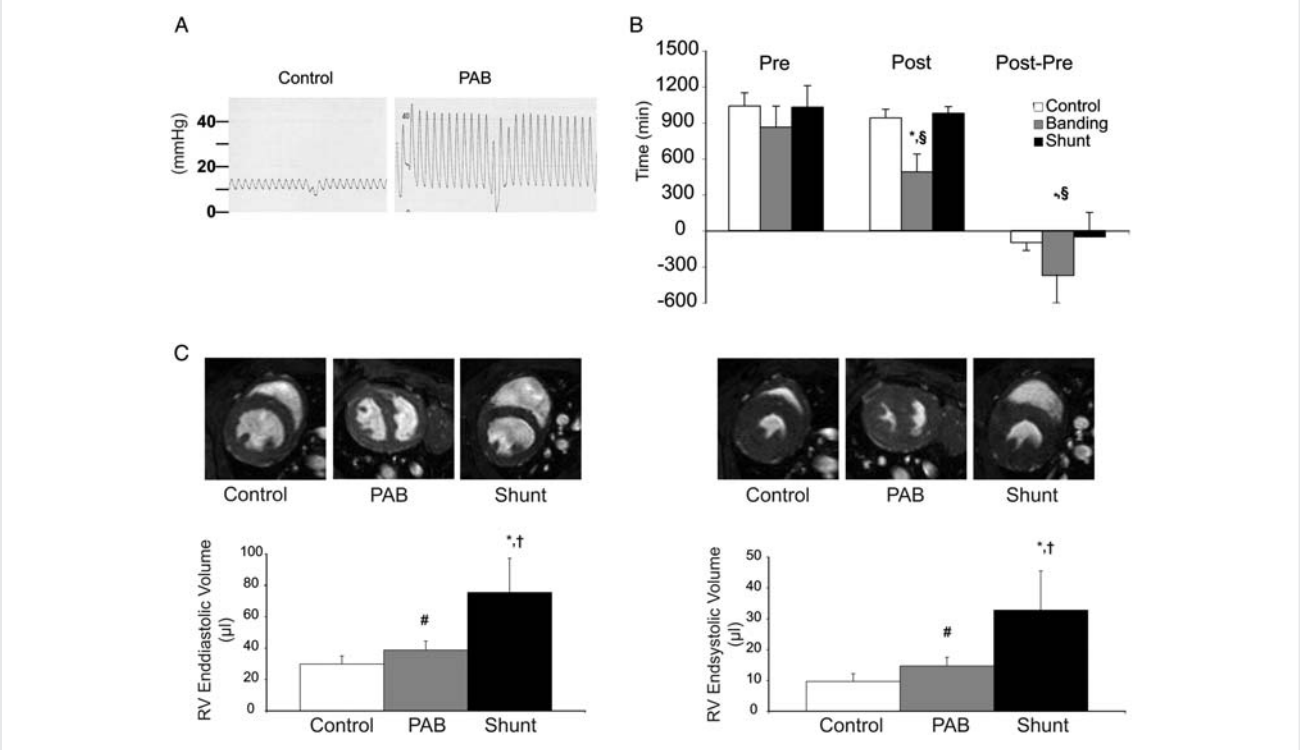

Figure 1 Functional adaptation to pressure or volume load of the right ventricle. (*A*) Typical examples of right ventricular pressure curves in a mouse without (left, Control) and with a PAB (right). Pressure is recorded in mmHg. (*B*) Voluntary cage wheel exercise in mice with PAB or Shunt time spent in the wheel before surgery (pre) and 3 weeks after surgery (post) in Control ($n = 8$), PAB ($n = 5$), and Shunt mice ($n = 5$). $^{*,\S}P < 0.05$ vs. Control and vs. Shunt. (*C*) Magnetic resonance imaging-derived right ventricular volumes: right ventricular end-diastolic (left) and end-systolic (right) volumes in microlitres. Typical short axis frames at the level of the papillary muscles from cardiac magnetic resonance imaging in the three groups are shown at the top. $N = 5$ for Control, $N = 6$ for PAB, and $N = 6$ for Shunt. $^{*}P < 0.05$ vs. Control, $^{\dagger}P < 0.05$ vs. PAB, $^{\#}t$-test Control vs. PAB $P = 0.026$, and 0.013 for right ventricular end-diastolic and right ventricular end-systolic volume, respectively. PAB, pulmonary artery banding.

(Shunt) had severe RV dilatation (*Figure 1C*), with increased RV SV and output (*Table 1*). Shunt mice had a decreased RV EF (*Table 1*). In PAB mice, LV volumes and LV output did not change. In Shunt mice, LV EDV and ESV were increased (*Table 1*). There were no significant differences in heart rate during MRI studies between the three groups (*Table 1*). Examples of cine loops are presented in the online data supplement. Right ventricular mass was significantly increased in mice with a PAB as well as in those with a Shunt (*Table 1*), which was confirmed at autopsy.

Pressure loading imposed a greater increase in energy demand on the RV than volume load, since RV stroke work was more increased in PAB mice than in Shunt mice (*Figure 2A*). Also, RV wall stress was only significantly increased in PAB mice (*Figure 2B*). Virtual pressure−volume loops derived from MRI and pressure measurements, showed a rightward and upward shift in the PAB mice but only a rightward shift in the Shunt mice (*Figure 2C*).

Cardiac remodelling

Both, PAB and Shunt induced similar degrees of RV hypertrophy: RV free wall weight was increased absolutely and relative to body weight (*Figure 3A*, *Table 2*). Shunt mice also showed increased septal weight, whereas PAB mice showed no change in septal weights (*Table 2*). Left ventricular-weight was not affected by PAB, whereas Shunt mice showed also increased LV weights (*Table 2*). Typical examples of Gomori-stained sections illustrate the RV hypertrophy in mice with a PAB or Shunt (*Figure 3B*). There was no significant increase in the expression of markers of cardiac fibrosis, i.e. collagen type 1 or 3 (Col1A2, Col3A1,[19] *Table 2*).

Despite the similar increase in RV hypertrophy in the pressure- and volume-loaded RVs, there were marked differences in molecular responses. Pulmonary artery banding induced a strong increase in typical markers of cardiac hypertrophy (*Figure 3C*), as shown by the increase in expression of natriuretic peptide A (NPPA), alpha 1 skeletal muscle actin (Acta1), and the decrease in alpha-Myosin Heavy Chain (MHC, myh6). In contrast, Shunt mice only showed moderate changes in expression of these markers.

The RV hypertrophy in the PAB mice was accompanied by a significant increase in expression of Modulatory Calcineurin Interacting Protein-1 (MCIP1), indicating calcineurin-activation, whereas MCIP1 was not significantly elevated in Shunt mice (*Figure 4A*). In the left ventricles of the PAB mice and Shunt mice there was no significant change in MCIP1 activation (*Figure 4A*). Pulmonary

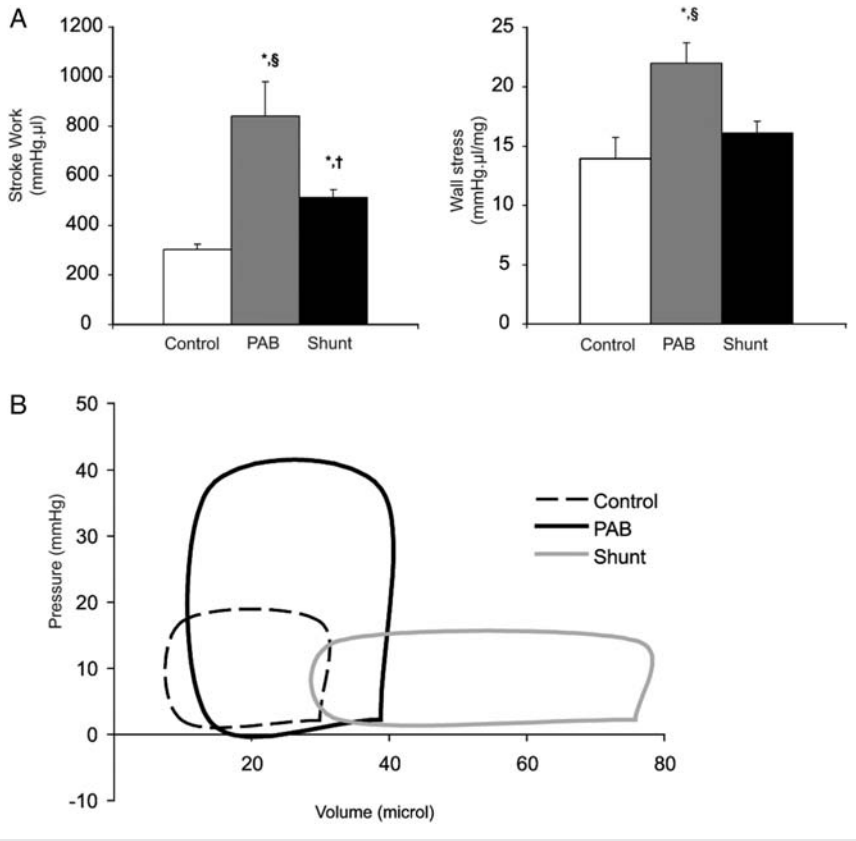

Figure 2 Haemodynamics. Calculated haemodynamics showed a higher increase in energy demand in the pressure-loaded right ventricle than in the volume-loaded right ventricle. (*A*) Stroke work was increased, more in PAB than in Shunt mice. (*B*) Wall stress was only increased in PAB mice. (*C*) Virtual pressure–volume loops derived from magnetic resonance imaging volumes (see methods). $N = 5$ for Control, $N = 6$ for PAB, and $N = 6$ for Shunt. $^{*}P < 0.05$ vs. Control, $^{\dagger}P < 0.05$ vs. PAB, $^{\S}P < 0.05$ vs. Shunt. PAB, pulmonary artery banding.

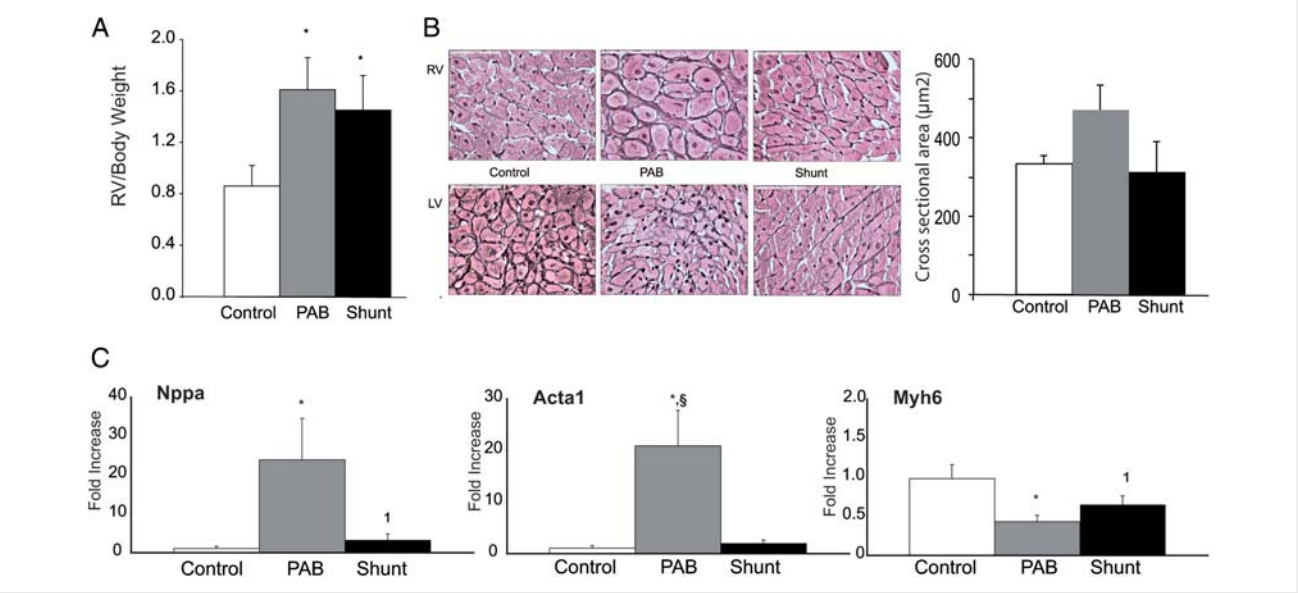

Figure 3 Morphological and molecular analysis of the right ventricle. (*A*) Right ventricular hypertrophy, expressed as right ventricular free wall (mg)/bodyweight (g) showed a similar increase in PAB and Shunt mice. $N = 22$ for Control, 12 for Shunt, and 10 for PAB. $^{*}P < 0.05$ vs. Control. (*B*) Left: typical example of Gomori-stained sections from right ventricular and left ventricular sections were visualized at $\times 40$ magnification. The scale bar represents 75 micrometers. Right: the cross-sectional area of the right ventricular myocytes. (*C*) Real-time polymerase chain reaction analysis for hypertrophic markers in the right ventricle. Cyclophilin was used as reference gene, expression in the control group was set to 1. $N = 4$ for each group. $^{*}P < 0.05$ vs. Control, $^{\S}P < 0.05$ vs. Shunt, $^{1}P = 0.06$ vs. Control. PAB, pulmonary artery banding.

Table 2 Cardiac weights and right ventricular gene expression

	Control	PAB	Shunt
N	22	10	12
Body weight (g)	23.6 ± 2.6	24.8 ± 1.4	25.3 ± 2.1
Heart weight (mg)	107 ± 11	131 ± 11*	169 ± 29*,†
RV (mg)	20 ± 5	40 ± 5*	37 ± 9*
Septum (mg)	20 ± 7	22 ± 5	35 ± 14*,†
LV (mg)	66 ± 8	70 ± 10	97 ± 15*,†
RV/(LV + S)	0.24 ± 0.06	0.44 ± 0.07*	0.28 ± 0.04
S/BW	0.91 ± 0.32	0.87 ± 0.22	1.49 ± 0.44*,†
HW/BW	4.59 ± 0.51	5.30 ± 0.49*	6.65 ± 0.89*,†
RV gene expression			
Beta/alpha-MHC	1.0 ± 0.1	19.0 ± 4.9*	4.6 ± 2.0
Col1A2	1.0 ± 0.1	1.6 ± 0.3	1.5 ± 0.5
Col3A1	1.0 ± 0.1	1.5 ± 0.3	0.7 ± 0.2

S, interventricular septum; BW, body weight; H, heart weight, which is the sum of the weights of RV free wall, interventricular septum, and LV free wall. Gene expression levels in the RV free wall were expressed as fold-increase vs. control mice.
$^{*}P < 0.05$ vs. Control, $^{\dagger}P < 0.05$ vs. PAB.

artery banding also induced a significant increase in beta-MHC (myh 7, *Figure 4B*) and a switch in beta/alpha-MHC ratio (*Table 2*). In the left ventricle, myh7 was also significantly increased after PAB (*Figure 4B*). In contrast, in the Shunt mice neither beta-MHC expression (*Figure 4B*) nor beta/alpha-MHC ratio (*Table 2*) were significantly increased in the right ventricle.

The amount of phosphorylated extracellular regulated kinase (ERK1/2), recently described as a switch to induce eccentric vs. concentric hypertrophy,[20] was decreased in the RV and LV of Shunt mice, in line with the response to increased pre-load. In the PAB mice, the amount of phosphorylated ERK1/2 was also decreased, possibly associated with the mild RV dilatation. The amount of phosphorylated Akt, a signalling pathway in physiological forms of hypertrophy,[21] was not significantly changed in the RV of mice with a PAB or Shunt, but tended to decrease in the LV of Shunt mice.

Discussion

In this study, we have demonstrated that mice with increased pressure or volume load of the RV develop similar degrees of RV hypertrophy but show different patterns of functional and molecular adaptation. Mice with a pressure-loaded RV (PAB) had reduced exercise capacity with moderately increased RV volumes, whereas SV was unchanged suggesting a harbinger of decompensating RV hypertrophy, anticipating clinical failure. The functional adaptation of the RV was coupled with an increase in MCIP1 expression, indicating calcineurin-activation, and a switch in MHC isoform ratio. In contrast, mice with a volume-loaded RV (Shunt) had normal exercise capacity, albeit with higher RV volumes and RV SVs at rest, indicating a pattern of adequately

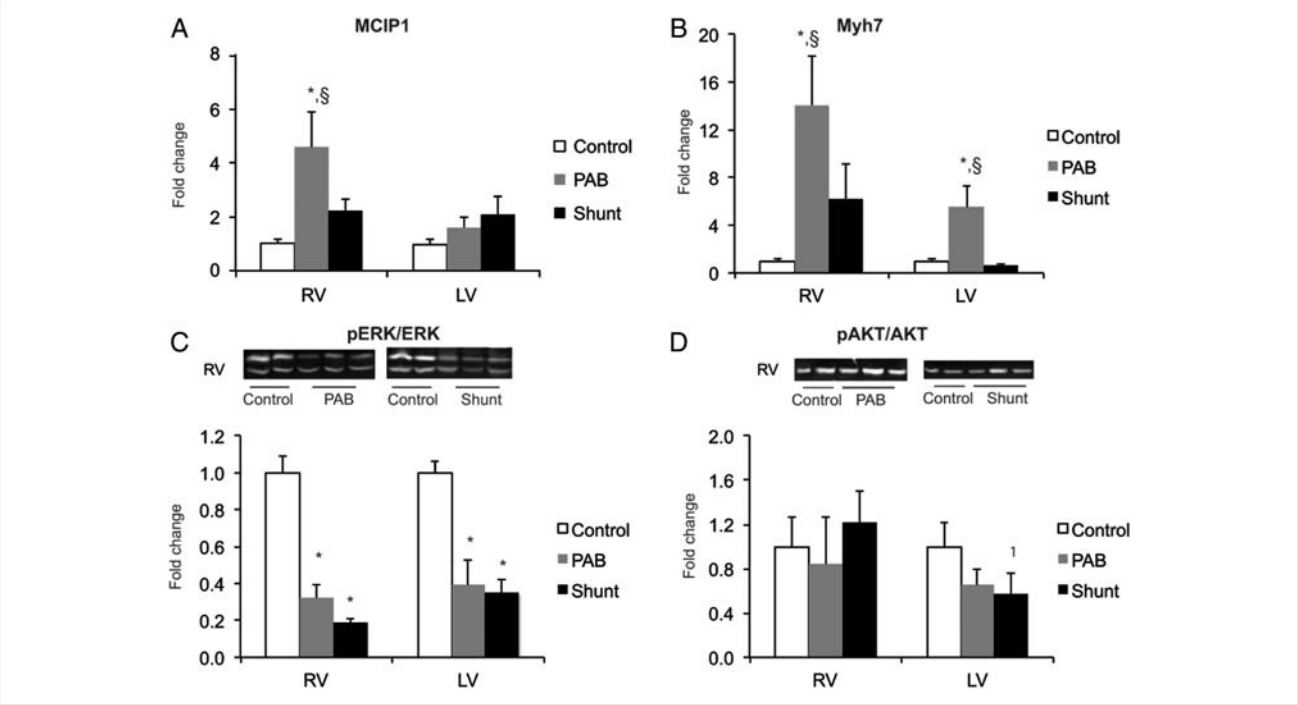

Figure 4 Calcineurin-activation and hypertrophy signalling. (*A*) Gene expression of Modulatory-Calcineurin-Interacting-Protein 1, a marker of calcineurin-activation, increased in the right ventricular free wall (RV) with pressure load (PAB), but not significantly with volume load (RV). LV = left ventricular free wall (LV), cyclophilin was used as reference gene. (*B*) Gene expression of beta-myosin heavy chain (myh7) increased in the right ventricle and left ventricle of PAB mice compared with cyclophilin as reference gene. (*C*) Protein levels of phosphorylated/total extra-cellular-regulated kinase decreased in the right ventricle and left ventricle. (*D*) Protein levels of phosphorylated/total Akt did not change in the right ventricle and decreased in the volume-loaded left ventricle. The data of the Control mice were set to 1. $N = 4$ in all groups. $^{*}P < 0.05$ vs. Control mice, $^{\S}P < 0.05$ vs. Shunt, $^{1}P = 0.06$ vs. right ventricle. PAB, pulmonary artery banding.

compensated RV hypertrophy. Moreover, in the RV of Shunt mice there was no significant MCIP-activation and only a mild change in MHC isoform ratio.

The pressure-loaded mice already worked at higher RV volumes measured with cardiac MRI, as was illustrated in the virtual pressure–volume loops. Previous studies with pulmonary banding in different species showed models in which RV volumes (assessed with conductance catheters or angiography) either did not change[14,22] or increased similarly.[23,24] However, none of these studies evaluated functional outcomes. From our studies it may be suggested that the pressure-loaded RV uses heterometric adaptation (Starling mechanism) to adapt and that given the reduced exercise tolerance this adaptation fell short in these mice. In contrast, in the volume-loaded mice, we showed a dramatic increase in RV volumes with normal functional adaptation.

This study showed a difference in functional adaptation to a volume vs. pressure load that also led to differences in 'clinical' outcome as assessed by exercise. Although nowadays it is recognized that longstanding volume load for the RV, such as pulmonary insufficiency after Fallot repair[1] leads to RV failure, pressure load appears to be more harmful as it leads to RV failure in a shorter time frame, through unknown mechanisms. It could be due to the higher RV stroke work with pressure load (*Figure 2*), leading to a higher metabolic demand and thereby changing mitochondrial potential which affects stress signalling.[25] Another possibility is that the fixed afterload of the PAB mice made them more dependent upon heart rate changes for the response to increased demands, as was recently also shown in patients with RV failure due to pulmonary hypertension.[26] The type of loading may also induce different molecular signalling patterns, which affect the RV response. Indeed, we showed a remarkable difference in calcineurin-activation, a known pathway of pathological hypertrophy in the left ventricle.[6] This difference was accompanied by a differential response in beta-MHC expression, part of a generalized hypertrophic response pattern to stress,[27] between volume and pressure load of the RV in mice. Since the calcineurin pathway has been successfully targeted in experimental and clinical left-sided heart failure,[28] these results suggest new targets for therapies to improve the pressure-loaded RV. For the volume-loaded RV, it is not yet known what mechanisms contribute to RV adaptation. Recently, it was suggested that in the LV with a volume load, early activation of the Akt-pathway may be responsible for a more physiological form of cell growth,[21] although the Akt-pathway has also been implicated in pathological hypertrophy in other studies.[29] After 4 weeks, we did not observe activation of the Akt-pathway anymore, which may be a time-related phenomenon. The eccentric hypertrophy classically described in volume-loaded hearts was recently suggested to be induced by

de-activation of the ERK1/2 pathway.[20] Our study confirms these results in the RV and LV of volume-loaded mice. Interestingly, in our mildly dilating pressure-loaded mice, we also observed a decrease in phosphorylated ERK1/2. This may be a secondary effect after the initial pressure response, possibly due to activation of dual-specificity phosphatase 6,[30] a known inhibitor of ERK-activation. De-activation of ERK could be a first sign of decompensation in the pressure-loaded mice,[30] and if so, prevention of ERK deactivation may be a strategy to prevent the pressure-loaded RV from dilation.

In this study, we showed a marked difference in cardiac remodelling between pressure and volume load in the RV. So far, treatment modalities for both the pressure-loaded RV as well as the volume-loaded RV are lacking. In studies in pressure-loaded LVs,[31] similar response patterns were seen as in the pressure-loaded RVs with respect to calcineurin-activation, suggesting that despite the difference in genetic make-up between the right and left ventricle,[9] the building blocks of the ventricle may be the same.[11] Hence, it may be inferred that strategies aimed at reducing calcineurin-activation may have a similar beneficial effect on the pressure-loaded RV as the pressure-loaded LV. In the volume-loaded RV, however, there appeared to be differences in activation of Akt and myh7 at 4 weeks, although the pathophysiological significance of these differences is as yet unclear. More studies into the cellular response of the RV to volume load are needed to clarify these issues and develop treatment strategies.

A limitation of this study is that the mice were evaluated at one time-point in the process of RV adaptation. Coupling of these functional outcomes to molecular signals at serial time-points after induction of the abnormal loading conditions may provide further understanding of these mechanisms of adaptation and dysfunction.

In conclusion, in this study we functionally characterized two mouse models of abnormal loading conditions of the right ventricle, that is increased pressure load and increased volume load. We demonstrated that mice with increased pressure and volume load of the RV developed similar degrees of RV hypertrophy, but showed differences in functional and molecular adaptation. Pressure load showed a pattern of adaptation suggesting a harbinger of decompensating RV hypertrophy accompanied by calcineurin-activation, whereas volume load induced a pattern of adequately compensated RV hypertrophy and no signs of calcineurin-activation. These findings may have important consequences for developing strategies to prevent RV failure in the abnormally loaded RV.

Supplementary material

Supplementary material is available at *European Journal of Heart Failure* online.

Funding

This work was supported by the Netherlands Heart Foundation (NHS2006T038) and the Sebald Foundation.

Conflict of interest: none declared.

References

1. Bouzas B, Kilner PJ, Gatzoulis MA. Pulmonary regurgitation: not a benign lesion. *Eur Heart J* 2005;**26**:433–439.
2. Norozi K, Wessel A, Alpers V, Arnhold JO, Geyer S, Zoege M, Buchhorn R. Incidence and risk distribution of heart failure in adolescents and adults with congenital heart disease after cardiac surgery. *Am J Cardiol* 2006;**97**:1238–1243.
3. Oechslin EN, Harrison DA, Connelly MS, Webb GD, Siu SC. Mode of death in adults with congenital heart disease. *Am J Cardiol* 2000;**86**:1111–1116.
4. Bourantas CV, Loh HP, Bragadeesh T, Rigby AS, Lukaschuk EI, Garg S, Tweddel AC, Alamgir FM, Nikitin NP, Clark AL, Cleland JG. Relationship between right ventricular volumes measured by cardiac magnetic resonance imaging and prognosis in patients with chronic heart failure. *Eur J Heart Fail* 2011;**13**:52–60.
5. Voelkel NF, Quaife RA, Leinwand LA, Barst RJ, McGoon MD, Meldrum DR, Dupuis J, Long CS, Rubin LJ, Smart FW, Suzuki YJ, Gladwin M, Denholm EM, Gail DB. Right ventricular function and failure: report of a National Heart, Lung, and Blood Institute working group on cellular and molecular mechanisms of right heart failure. *Circulation* 2006;**114**:1883–1891.
6. Wilkins BJ, Dai YS, Bueno OF, Parsons SA, Xu J, Plank DM, Jones F, Kimball TR, Molkentin JD. Calcineurin/NFAT coupling participates in pathological, but not physiological, cardiac hypertrophy. *Circ Res* 2004;**94**:110–118.
7. van Rooij E, Doevendans PA, Crijns HJ, Heeneman S, Lips DJ, van Bilsen M, Williams RS, Olson EN, Bassel-Duby R, Rothermel BA, De Windt LJ. MCIP1 overexpression suppresses left ventricular remodeling and sustains cardiac function after myocardial infarction. *Circ Res* 2004;**94**:e18–e26.
8. Ho SY, Nihoyannopoulos P. Anatomy, echocardiography, and normal right ventricular dimensions. *Heart* 2006;**92**(Suppl 1):i2–i13.
9. Srivastava D. Making or breaking the heart: from lineage determination to morphogenesis. *Cell* 2006;**126**:1037–1048.
10. Zaffran S, Kelly RG, Meilhac SM, Buckingham ME, Brown NA. Right ventricular myocardium derives from the anterior heart field. *Circ Res* 2004;**95**:261–268.
11. Olson EN. Gene regulatory networks in the evolution and development of the heart. *Science* 2006;**313**:1922–1927.
12. Haddad F, Hunt SA, Rosenthal DN, Murphy DJ. Right ventricular function in cardiovascular disease, part I: anatomy, physiology, aging, and functional assessment of the right ventricle. *Circulation* 2008;**117**:1436–1448.
13. Bar H, Kreuzer J, Cojoc A, Jahn L. Upregulation of embryonic transcription factors in right ventricular hypertrophy. *Basic Res Cardiol* 2003;**98**:285–294.
14. Faber MJ, Dalinghaus M, Lankhuizen IM, Steendijk P, Hop WC, Schoemaker RG, Duncker DJ, Lamers JM, Helbing WA. Right and left ventricular function after chronic pulmonary artery banding in rats assessed with biventricular pressure-volume loops. *Am J Physiol Heart Circ Physiol* 2006;**291**:H1580–H1586.
15. Tarnavski O, McMullen JR, Schinke M, Nie Q, Kong S, Izumo S. Mouse cardiac surgery: comprehensive techniques for the generation of mouse models of human diseases and their application for genomic studies. *Physiol Genomics* 2004;**16**:349–360.
16. Mori T, Chen YF, Feng JA, Hayashi T, Oparil S, Perry GJ. Volume overload results in exaggerated cardiac hypertrophy in the atrial natriuretic peptide knockout mouse. *Cardiovasc Res* 2004;**61**:771–779.
17. van Albada ME, Schoemaker RG, Kemna MS, Cromme-Dijkhuis AH, van Veghel R, Berger RM. The role of increased pulmonary blood flow in pulmonary arterial hypertension. *Eur Respir J* 2005;**26**:487–493.
18. Buitrago M, Lorenz K, Maass AH, Oberdorf-Maass S, Keller U, Schmitteckert EM, Ivashchenko Y, Lohse MJ, Engelhardt S. The transcriptional repressor Nab1 is a specific regulator of pathological cardiac hypertrophy. *Nat Med* 2005;**11**:837–844.
19. Schafer S, Ellinghaus P, Janssen W, Kramer F, Lustig K, Milting H, Kast R, Klein M. Chronic inhibition of phosphodiesterase 5 does not prevent pressure-overload-induced right-ventricular remodelling. *Cardiovasc Res* 2009;**82**:30–39.
20. Kehat I, Davis J, Tiburcy M, Accornero F, Saba-El-Leil MK, Maillet M, York AJ, Lorenz JN, Zimmermann WH, Meloche S, Molkentin JD. Extracellular signal-regulated kinases 1 and 2 regulate the balance between eccentric and concentric cardiac growth. *Circ Res* 2010;**108**:176–183.
21. Toischer K, Rokita AG, Unsold B, Zhu W, Kararigas G, Sossalla S, Reuter SP, Becker A, Teucher N, Seidler T, Grebe C, Preuss L, Gupta SN, Schmidt K, Lehnart SE, Kruger M, Linke WA, Backs J, Regitz-Zagrosek V, Schafer K, Field LJ, Maier LS, Hasenfuss G. Differential cardiac remodeling in preload versus afterload. *Circulation* 2010;**122**:993–1003.
22. Gaynor SL, Maniar HS, Bloch JB, Steendijk P, Moon MR. Right atrial and ventricular adaptation to chronic right ventricular pressure overload. *Circulation* 2005;**112**(9 Suppl):I212–I218.
23. Hessel MH, Steendijk P, den Adel B, Schutte CI, van der Laarse A. Characterization of right ventricular function after monocrotaline-induced pulmonary hypertension in the intact rat. *Am J Physiol Heart Circ Physiol* 2006;**291**:H2424–H2430.

24. Rockman HA, Ono S, Ross RS, Jones LR, Karimi M, Bhargava V, Ross J Jr, Chien KR. Molecular and physiological alterations in murine ventricular dysfunction. *Proc Natl Acad Sci USA* 1994;**91**:2694–2698.
25. Michelakis ED. Mitochondrial medicine: a new era in medicine opens new windows and brings new challenges. *Circulation* 2008;**117**:2431–2434.
26. Groepenhoff H, Westerhof N, Jacobs W, Boonstra A, Postmus PE, Vonk-Noordegraaf A. Exercise stroke volume and heart rate response differ in right and left heart failure. *Eur J Heart Fail* 2010;**12**:716–720.
27. Chien KR, Zhu H, Knowlton KU, Miller-Hance W, van-Bilsen M, O'Brien TX, Evans SM. Transcriptional regulation during cardiac growth and development. *Annu Rev Physiol* 1993;**55**:77–95.
28. da Costa Martins PA, Salic K, Gladka MM, Armand AS, Leptidis S, el Azzouzi H, Hansen A, Coenen-de Roo CJ, Bierhuizen MF, van der Nagel R, van Kuik J, de Weger R, de Bruin A, Condorelli G, Arbones ML, Eschenhagen T, De Windt LJ. MicroRNA-199b targets the nuclear kinase Dyrk1a in an auto-amplification loop promoting calcineurin/NFAT signalling. *Nat Cell Biol* 2010;**12**:1220–1227.
29. Bonnet S, Paulin R, Sutendra G, Dromparis P, Roy M, Watson KO, Nagendran J, Haromy A, Dyck JR, Michelakis ED. Dehydroepiandrosterone reverses systemic vascular remodeling through the inhibition of the Akt/GSK3-{beta}/NFAT axis. *Circulation* 2009;**120**:1231–1240.
30. Purcell NH, Wilkins BJ, York A, Saba-El-Leil MK, Meloche S, Robbins J, Molkentin JD. Genetic inhibition of cardiac ERK1/2 promotes stress-induced apoptosis and heart failure but has no effect on hypertrophy in vivo. *Proc Natl Acad Sci USA* 2007;**104**:14074–14079.
31. Vega RB, Rothermel BA, Weinheimer CJ, Kovacs A, Naseem RH, Bassel-Duby R, Williams RS, Olson EN. Dual roles of modulatory calcineurin-interacting protein 1 in cardiac hypertrophy. *Proc Natl Acad Sci USA* 2003;**100**:669–674.